metals

MDPI

Article

Prediction of Dimensional Changes of Low-Cost Metal Material Extrusion Fabricated Parts Using Machine Learning Techniques

Zhicheng Zhang [1], James Femi-Oyetoro [1], Ismail Fidan [2,*], Muhammad Ismail [3] and Michael Allen [4]

[1] Department of Mechanical Engineering, Tennessee Tech University, Cookeville, TN 38505, USA; zzhang44@tntech.edu (Z.Z.); jdfemioyet42@tntech.edu (J.F.-O.)
[2] Department of Manufacturing and Engineering Technology, Tennessee Tech University, Cookeville, TN 38505, USA
[3] Department of Computer Science, Tennessee Tech University, Cookeville, TN 38505, USA; mismail@tntech.edu
[4] Department of Mathematics, Tennessee Tech University, Cookeville, TN 38505, USA; mallen@tntech.edu
* Correspondence: ifidan@tntech.edu; Tel.: +1-(931)-372-6298

Abstract: Additive manufacturing (AM) is a layer-by-layer manufacturing process. However, its broad adoption is still hindered by limited material options, different fabrication defects, and inconsistent part quality. Material extrusion (ME) is one of the most widely used AM technologies, and, hence, is adopted in this research. Low-cost metal ME is a new AM technology used to fabricate metal composite parts using sintered metal infused filament material. Since the involved materials and process are relatively new, there is a need to investigate the dimensional accuracy of ME fabricated metal parts for real-world applications. Each step of the manufacturing process, from the material extrusion to sintering, might significantly affect the dimensional accuracy. This research provides a comprehensive analysis of dimensional changes of metal samples fabricated by the ME and sintering process, using statistical and machine learning algorithms. Machine learning (ML) methods can be used to assist researchers in sophisticated pre-manufacturing planning and product quality assessment and control. This study compares linear regression to neural networks in assessing and predicting the dimensional changes of ME-made components after 3D printing and sintering process. In this research, the ML algorithms present a significantly high coefficient of determination (i.e., 0.999) and a very low mean square error (i.e., 0.0000878). The prediction outcomes using a neural network approach have the smallest mean square error among all ML algorithms and it has quite small p-values. So, in this research, the neural network algorithm has the highest accuracy. The findings of this study can help researchers and engineers to predict the dimensional variations and optimize the printing and sintering process parameters to obtain high quality metal parts fabricated by the low-cost ME process.

Keywords: low-cost metal material extrusion; additive manufacturing; machine learning; dimensional accuracy; sintering

Citation: Zhang, Z.; Femi-Oyetoro, J.; Fidan, I.; Ismail, M.; Allen, M. Prediction of Dimensional Changes of Low-Cost Metal Material Extrusion Fabricated Parts Using Machine Learning Techniques. *Metals* **2021**, *11*, 690. https://doi.org/10.3390/met11050690

Academic Editors: Chris Aldrich, Thomas Niendorf and Mohammed Nouari

Received: 24 February 2021
Accepted: 20 April 2021
Published: 23 April 2021

1. Introduction

Additive manufacturing (AM), also known as 3D printing (3DP) [1], is a set of technologies that are used to produce objects layer-by-layer from computer-aided design (CAD) models [2]. There are various types of AM processes including material extrusion (ME), selective laser sintering (SLS), selective laser melting (SLM), powder bed fusion (PBF), and stereolithography (STL) [3]. Among these techniques, ME is well-known and the most widely used process [4]. ME has plenty of advantages over traditional manufacturing methods such as the production of highly complex parts with less weight, time, and material cost [5]. The research of the ME process is growing sharply in plenty of areas, such as medicine [6], construction [7], machinery manufacturing [8], and the food industry [9]. Recently, ME has been used in the manufacturing of metal components [10]. In recent

years, new metal-infused polymer filaments have been developed as a feedstock material for ME process and can be used to fabricate metal components using this new, low-cost manufacturing processes [11].

Sintering is a process that forms a solid mass of metal by heating the composite material of metal powder and a binding agent to just below the melting point of the metal [12]. The metal-polymer composite filament is melted and extruded in the 3D printer then sintered to change the metal-polymer composite parts to pure metal [13]. 3D printed metal-composite parts need to be sintered in order to melt the polymer and diffuse the metal particles inside the polymer matrix material. After sintering, the internal polymer will melt and the metal material will glue together. Moreover, the sintering process is crucial, because the mechanical properties of the metal-polymer composite parts are much lower than pure metal [14]. In this context, by heating the metal-polymer composite parts to just below the melting temperature of the metal, the polymer will melt and evaporate slowly, which eventually will lead to having a pure metal component [15]. It has been shown by the Gong's group and the Burkhardt's group that after the sintering process, the dimensions of the samples will change [11,16]. Thus, an accurate method is required to predict the CAD dimension.

The dimensional accuracy of AM has been studied by plenty of research groups. Yasa et al. studied the dimensional accuracy and mechanical properties of chopped carbon-fiber-reinforced, tough nylon productions, which were made by the ME method [17]. Osman et al. investigated the dimensional errors of AM fabricated samples by laser sintering [18]. The authors concluded that the precision of both selective laser sintering and 3DP models are acceptable. Ibrahim et al. analyzed the dimensional error in some AM methods [19]. They reported different dimensional errors and chose the most accurate one. In the research by Wang's group, they investigated the shrinkage caused by sintering process in the binder jetting AM technique [20]. Three sets of recommended sintering parameters were analyzed to achieve the best dimensional accuracy for each axis and one parameter in all three axes by Wang's group. Four sets of optimal sintering parameters were found by this research group to improve the dimensional accuracy.

Machine Learning (ML) is a subset of artificial intelligence, which can be used to predict mechanical properties of manufacturing parts [21]. ML can perform modeling and analysis on big data [22] to assist humans in various areas of technology such as language detection and translation [23], facial expression and motion analysis [24], medicine [25], etc. In recent years, ML has gained increasing attention in the AM field due to the application of regression, classification, and clustering. ML has numerous applications such as the prediction of tensile strength of Polylactic acid (PLA) objects fabricated by ME [22], design of AM [23], improvement of the geometrical accuracy fabricated by ME [24], etc. Although the dimensional accuracy of AM has been studied in plenty of works [25–28], ML was not used in these works, since their datasets are not large enough. For example, Gong's group used only 11 samples to get their results. Thus, there is a need for a large dataset to predict the dimensional accuracy in the low-cost metal ME process using ML techniques.

In this study, cuboid samples were fabricated by ME and the dimensions before and after sintering of the samples were collected. This study compares linear regression to neural networks in assessing and predicting the dimensional changes of ME made components after 3DP and sintering. These algorithms were used to predict the CAD dimensions of the samples based on the final sintered dimensions.

2. Materials and Methods

2.1. Materials and Equipment

In this research, the bronze-PLA filament made by The Virtual Foundry (Stoughton, WI, USA) [29] was used to print the non-sintered parts and fabricated in an Ultimaker S5 3D printer which is made by Ultimaker (Utrecht, The Netherlands) [30]. The sintering process was performed with the use of a KSL-1100X muffle furnace, made by the MTI Corporation (Richmond, CA, USA) [31]. A 35-025 electronic micrometer which is made by

iGaging (San Clemente, California, USA) [32], was used to take the measurement of the dimensions before and after the sintering process. The materials and equipment used in this research are shown in Figure 1. Figure 2 shows the metal-composite part as a CAD model, 3D printed and after sintering. The CAD model will be sliced in the software Cura, which is developed by Ultimaker too. This will keep the accuracy of printing process as much as possible.

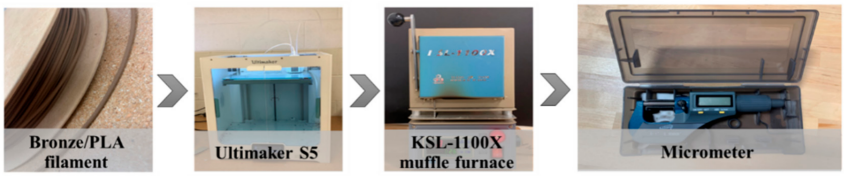

Figure 1. Material and equipment used in this research.

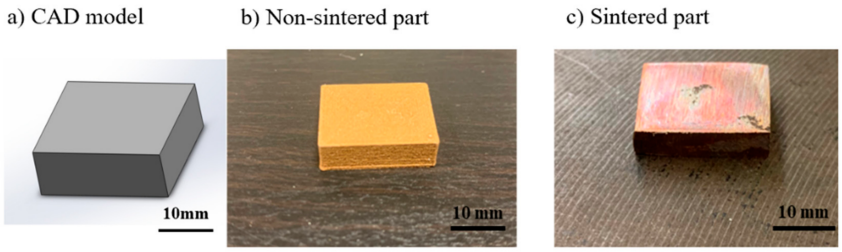

Figure 2. Samples in different status (**a**) CAD model (**b**) Bronze-PLA sample (**c**) sample after sintering and polishing.

2.2. Process Workflow

The schematic of this research is shown in Figure 3. There are three main sections in the research. The first section is the data collection. The g-code was generated from a CAD model in the slicing software, which then is used to fabricate the non-sintered parts in the 3D printer. After measuring the non-sintered dimensions, the non-sintered parts were sintered in the muffle furnace. After sintering, the sintered parts were polished and then measured. The second section is prediction. Prediction algorithms were trained, tested, and evaluated using the collected data. The third section is verification, where the performance of the prediction algorithm is validated via experimental results.

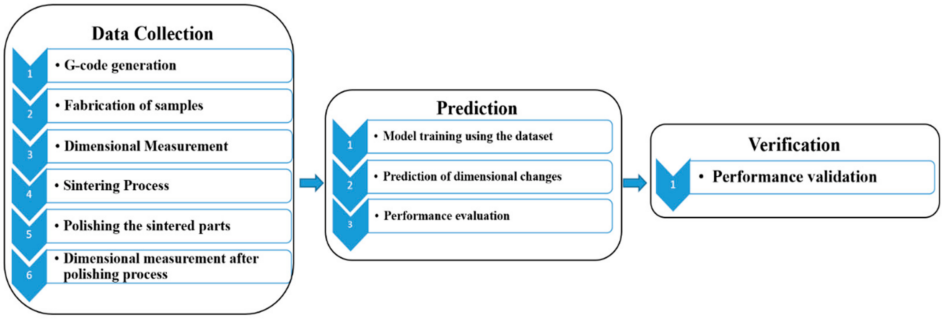

Figure 3. Process workflow of the research study.

2.3. Dataset Preparation

In this research, there are three different types of data, dimensions obtained from the CAD model, the non-sintered part, and the sintered and polished part. Since the dimensions of the final part are what is wanted, the regression and ML algorithms were developed to use the sintered dimensions with the various printing and sintering parameters to predict the starting CAD dimensions. The CAD dimensions can be controlled by the users in slicing

software and the non-sintered and sintered dimensions were measured by an iGaging micrometer.

From the printing process, layer thickness (the height of each layer during the printing process), nozzle temperature, and printing speed were chosen as explanatory variables. For the sintering process, sintering temperature, and ramp ratio (temperature increasing ratio) were chosen as the explanatory variables. The parameters of the printing and sintering process are given in Tables 1 and 2.

Table 1. Parameters of the printing process.

Printing Parameters	Values		
Layer Thickness (mm)	0.1	0.2	0.3
Nozzle Temperature (°C)	220	230	240
Printing Speed (mm/s)	10	15	20

Table 2. Parameters of the sintering process.

Sintering Parameters	Values						
Layer Thickness (mm)		0.1		0.2		0.3	
Sintering Temperature (°C)	870	875	880	885	890	895	900
Ramp Ratio (°C/min)		2		3		4	

In this research, 150 samples were fabricated and resulted in 450 groups of data points. Table 3 shows an example of the combination of the process parameters and their relationship with the sample dimensions. The part was printed with a layer thickness of 0.1 mm, 240 °C as nozzle temperature and a 10 mm/s printing speed. The sample was sintered in at 870 °C and the temperature increasing ratio is 2 °C/min. The CAD dimensions of the part are 20mm × 15mm × 6 mm, but after printing, the real dimensions of the part are bigger than the CAD. During the sintering process, the part undergoes a shrinkage process that reduces the dimensions to below CAD dimensions. Thus, compared to the CAD dimensions, the final dimensions will be significantly different. Therefore, a prediction of the CAD dimensions is needed.

Table 3. Combination of the process parameters.

Printing Parameters	Sintering Parameters	Sample Type	Dimensions of the Sample		
			Length (mm)	Width (mm)	Height (mm)
0.1 mm 240 °C 10 mm/s	0.1 mm 870 °Ca 2 °C/mm	CAD	20	15	6
		Non-sintered	20.452	15.318	6.226
		Sintered	18.787	13.922	5.236

2.4. Prediction Algorithms

The three types of algorithms used in this research were single linear regression (LR), linear regression with interactions (LRI) and Neural Networks (NN). All ML algorithms are developed in Python. The following subsections will explain the definitions and reasons of choosing these three kinds of algorithms.

2.4.1. LR

LR is a type of supervised ML algorithm that is used to predict continuous outcomes using a constant slope [33]. Since there are 8 independent variables, the polynomial regression is not a suitable method. LR is used in this research because of its briefness on

learning and using, accuracy in multiple variables, and reliability [34]. In this research, multiple features are used to do prediction and the equation of the LR is:

$$\mathbf{y} = \mathbf{X}\theta + \varepsilon \quad (1)$$

Here, **y** is the vector of response variables, **X** is the matrix of independent variables, θ is the coefficient vector, and ε is the vector of the error term. In this research, the CAD dimension is the response variable. The 8 independent variables are layer thickness (LT), sintering temperature (ST), ramp ratio (RR), nozzle temperature (NT), printing speed (PS) and the final length (L), width (W), and height (H). The LR algorithm will generate the θ and ε and the matrix of independent variables X is shown below:

$$\mathbf{X} = [\mathbf{LT} \quad \mathbf{ST} \quad \mathbf{RR} \quad \mathbf{NT} \quad \mathbf{PS} \quad \mathbf{L} \quad \mathbf{W} \quad \mathbf{H}] \quad (2)$$

2.4.2. LRI

LRI is a kind of unique linear regression method. Among the independent variables, there might be some interactions. LRI will involve these interactions during the analysis process [35] but LR does not. The equation of the LRI is the same as LR:

$$\mathbf{y} = \mathbf{X}\theta + \varepsilon \quad (3)$$

Here, **y** is the vector of response variables, **X** is the matrix of independent variables, θ is the coefficient vector and ε is the vector of the error term. In this research, the CAD dimension is the response variable. However, the matrix of independent variables X is different, The **X** for LRI is shown below:

$$\begin{aligned}\mathbf{X} = [&\mathbf{LT\ ST\ RR\ NT\ PS\ L\ W\ H\ LT \times L\ LT \times W\ LT \times H\ ST \times L\ ST \times W\ ST \times H}\\ &\mathbf{RR \times L\ RR \times W\ RR \times H\ NT \times L\ NT \times W\ NT \times H\ PS \times L\ PS \times W\ PS \times H}]\end{aligned} \quad (4)$$

2.4.3. NN

NN is a kind of ML algorithm which uses a set of network layers to translate an input data into an output [36]. NN uses multiple layers of linear processing units for feature extraction and transformation. Each layer uses the output from the previous layer as input, learning in supervised or unsupervised manners [37]. In this research, supervised manners are used since the response variables are labeled data. Also, a deep NN model is developed since we will involve more than a single hidden layer. The schematic of the NN is represented in Figure 4, starting at the input layer, the CAD dimensions, sintered dimensions, printing parameters, and sintering parameters are all inputted and data is analyzed in the hidden layers and then output. The output of the NN is the CAD dimensions, the inputs are the sintered data and printing/sintering parameters.

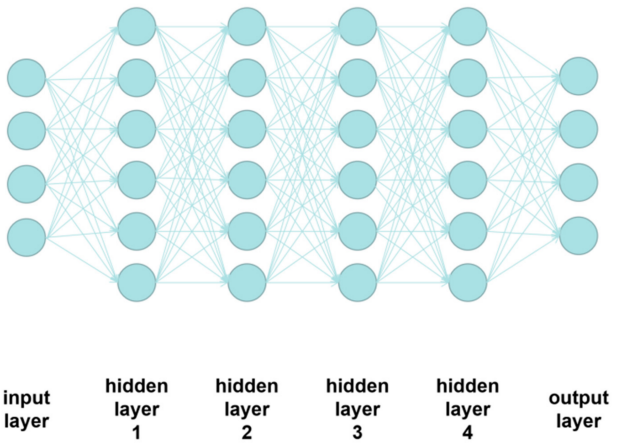

Figure 4. Schematic of the NN [38].

3. Results and Discussions

In this section, the results collected from the two different algorithms adopted in this paper are shown by figures presented. Firstly, the printing accuracy of the 3D printer is shown. Then, the dimensional changes between the CAD and sintered data were analyzed by LR, LRI and NN algorithms. The results from the three analysis algorithms adopted in this paper are presented.

3.1. Printing Accuracy

The errors between the non-sintered and CAD data are shown in Figure 5. The medians of all dimensional errors are not zero, which means that after printing, the non-sintered and CAD data are different. For the length and the width, non-sintered dimensions are larger than the CAD dimensions, which means that the real parts will expand in length and width than the 3D models after the printing process. As for the height, the real parts will shrink or expand than the 3D models.

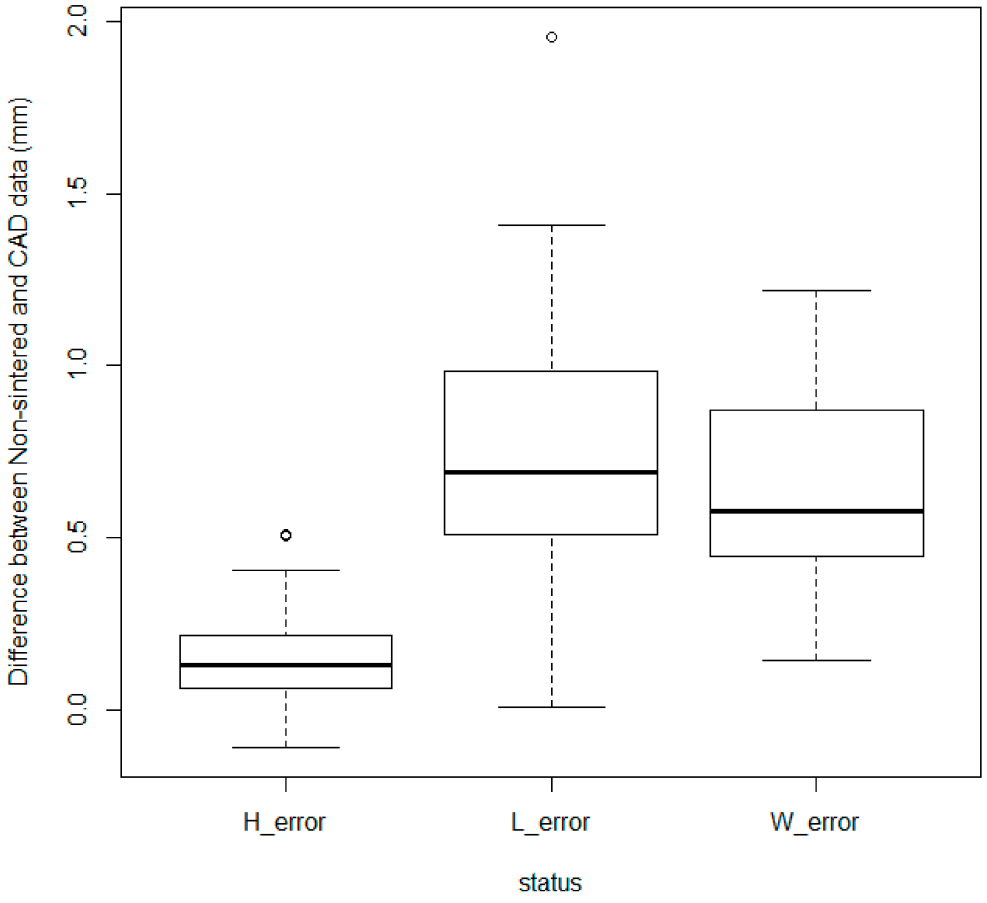

Figure 5. Difference between non-sintered and CAD data.

In the AM design process, the CAD dimensions can be controlled by the users. Thus, it is required to predict the CAD data, but not the non-sintered data.

3.2. Analysis of Dimensional Variations of CAD and Sintered Samples

In this subsection, the results of the prediction of CAD dimensions of three different algorithms are shown separately.

3.2.1. Results of Prediction by LR

After parameter optimization, the equations to predict the initial CAD dimensions by LR are:

$$\mathbf{CAD\_L = X \times [-0.000220\ 0.0649\ 0.0136\ 0.000300\ -0.0321\ 0.647\ 0.118\ 0.0793]^T + [-0.0231]} \quad (5)$$

$$\mathbf{CAD\_W = X \times [-0.00733\ 0.0698\ 0.0134\ -0.0364\ -0.100\ 0.250\ 0.556\ 0.0801]^T + [0.0260]} \quad (6)$$

$$\mathbf{CAD\_H = X \times [-0.00146\ 0.0633\ 0.0121\ -0.00729\ -0.0517\ 0.517\ 0.219\ 0.0757]^T + [-0.0154]} \quad (7)$$

The coefficients vector generated from the LR algorithm multiply the independent matrix will result in the prediction vector of CAD dimensions. Compared with the real CAD dimension vector, the error is shown in Figure 6. The medians of all three errors are close to zero and most absolute values of maximum and minimum errors are less than 1 mm, which means that in predicting most dimensions, LR is accurate. However, for length and width, there are also several outliers of 2 and 1.5 mm, respectively.

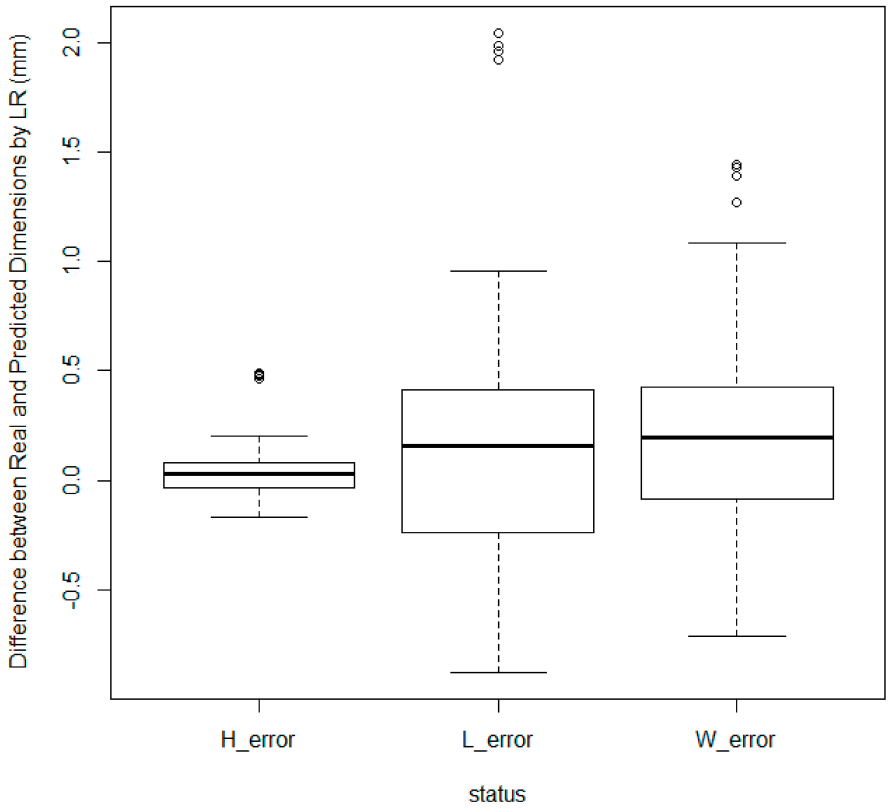

Figure 6. Difference between real and predicted CAD dimensions by LR.

3.2.2. Results of Prediction by LRI

After parameter optimization, the equations to predict the initial CAD dimensions by LRI are:

$$\mathbf{CAD\_L = X \times [-0.013\ 1.112\ 0.330\ -0.613\ -0.322\ -2.639\ 14.514\ 1.281\ 0.558\ -0.660\ 0.104\ 7.394\ -28.133\ 0.787\ -0.100\ -0.386\ 0.119\ -6.460\ 16.737\ -1.964\ 2.305\ -2.122\ 0.010]^T + [-0.317]} \quad (8)$$

$$\mathbf{CAD\_W = X \times [-0.099\ 1.354\ 0.505\ -0.690\ 0.153\ -15.797\ 30.514\ 4.166\ 0.400\ -0.451\ 0.165\ 10.959\ -36.130\ 0.808\ -0.108\ -0.606\ 0.138\ 4.270\ 8.337\ -4.605\ 0.917\ -1.459\ 0.047]^T + [-0.607]} \quad (9)$$

$$\mathbf{CAD\_H = X \times [-0.124\ 1.134\ 0.294\ -0.582\ -0.189\ -1.156\ 10.964\ 3.391\ 0.773\ -0.718\ 0.121\ 7.144\ -28.264\ 0.822\ -0.132\ -0.307\ 0.119\ -7.583\ 20.620\ -4.016\ 1.923\ -2.281\ 0.290]^T + [-0.431]} \quad (10)$$

The error between the prediction of CAD dimensions by the LRI and the real CAD dimensions is shown in Figure 7. The medians of all three errors are close to zero and most absolute values of maximum and minimum errors are less than 0.8 mm, which means that most predictions done by LRI are accurate and the variations of LRI predictions are smaller than LR predictions. In addition to length and width, there are also several outliers of 1.4 and 1.2 mm, respectively.

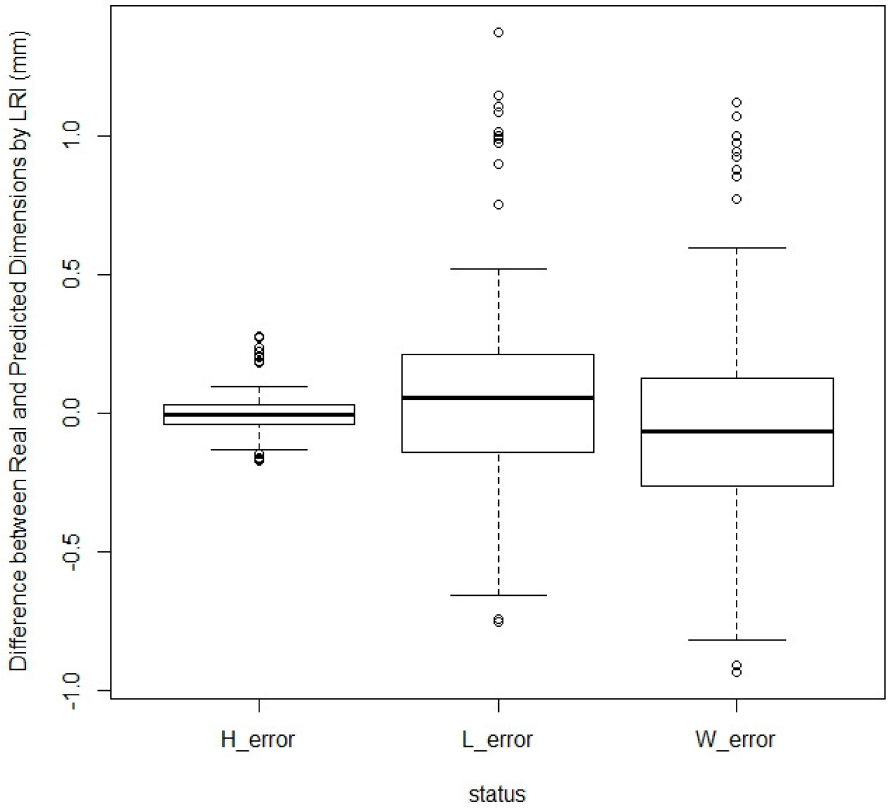

Figure 7. Difference between real and predicted CAD dimensions by LRI.

3.2.3. Results of Prediction by NN

After Hyper-parameter optimization, the depth (number of hidden layer), width (number of neurons per hidden layer), and activation function at hidden layers are generated and the structure of the NN is shown in Table 4.

Table 4. Structure of the NN.

Number of hidden layers	5
Number of neurons in each hidden layer	128
Activation function at hidden layers	ReLU

The test size of this NN model is 0.32, 144 groups of data are used in each run of the training process and the model is trained 500 times. All manufacturing parameters are independent variables in the input of the NN model; if any one of the parameters were deleted, the accuracy would be lower. In Figure 8, the results generated by NN are shown. The medians of all three errors are close to zero and most absolute values of maximum and minimum errors are less than 0.1 mm, which means NN is accurate and has the smallest variations among all three algorithms. For length and width, there are also several outliers but most of them are less than 0.4 mm. Compared to LR and LRI, NN is more accurate. As seen by the variance of NN is being smaller than LR and LRI. This can be attributed to the fact that NN can extract complex features within the data and hence yield better results compared with LR and LRI.

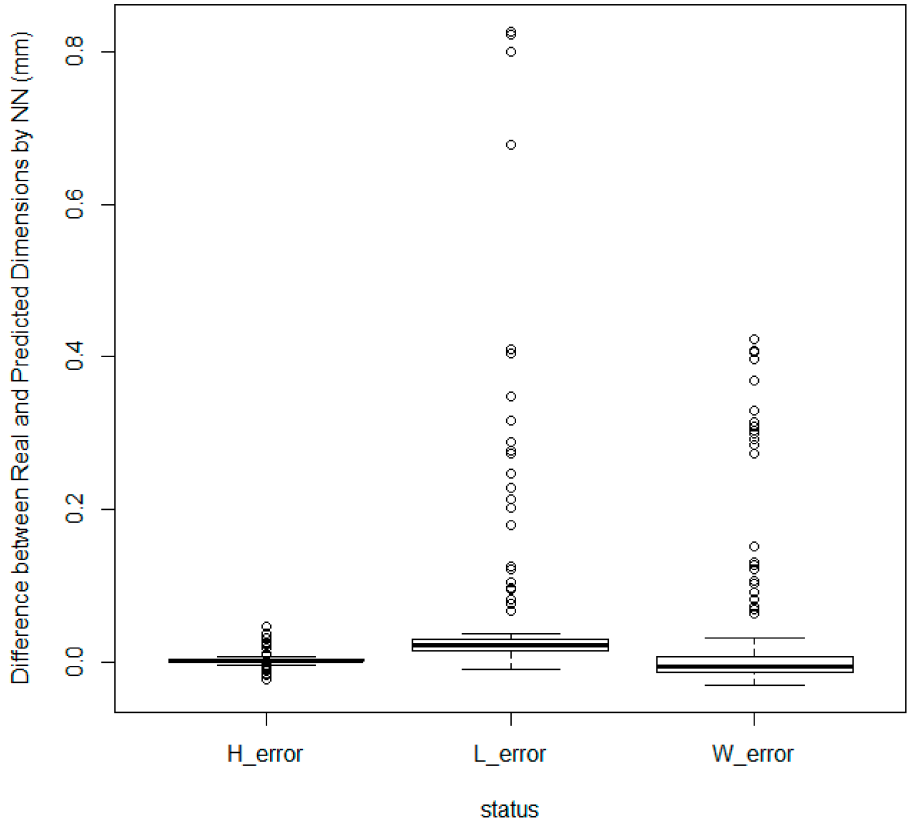

Figure 8. Difference between real and predicted CAD dimensions by NN.

In statistics, the p-value is usually used to evaluate the probability of extreme outcomes [39]. A very small p-value means that an extreme observed outcome would unlikely occur. Table 5 shows the p-values of NN-predicted length, width, and height. All p-values are significantly small.

Table 5. P-values of NN-predicted dimensions.

Dimensions	Length	Width	Height
p-value	2.99×10^{-8}	1.097×10^{-4}	1.272×10^{-6}

4. Error Metrics

The results of different algorithms have been shown in figures. It is difficult to test the performance from the figures. Models that are used to predict output values must have metrics to assess the performance or the success of the algorithm. There are several error metrics that are utilized in the ML community. In this research, the coefficient of determination (R^2) values and mean square error (MSE) metrics was used to test the performance of the algorithms.

R^2 is the proportion of the variance in the dependent variable that is predictable from the independent variable [40]. The equation is given below:

$$R^2 = 1 - \mathrm{RSS}/\mathrm{TSS} \tag{11}$$

where the RSS is sum of squares of residuals and TSS is total sum of squares.

MSE is the average squared difference between the estimated values (predicted values) and the actual value (observed values) [41]. The equation is given below:

$$\boldsymbol{MSE} = \frac{\mathbf{1}}{\boldsymbol{n}} \sum_{\boldsymbol{i}=\mathbf{1}}^{\boldsymbol{n}} \left(\boldsymbol{Y_i} - \hat{\boldsymbol{Y}}_{\boldsymbol{i}}\right)^{\mathbf{2}} \tag{12}$$

where MSE is the mean square error, n is the sample size used to test an algorithm, Y_i is the observed value, and $\hat{Y}_i$ is the value predicted by the algorithm.

The R^2s of LR and LRI are shown in Table 6. LRI has a larger R^2 than LR. So, the correlation of LRI is more reliable than LR.

Table 6. R^2 results.

Method	R^2 Value		
	Length	**Width**	**Height**
LR	0.891	0.921	0.885
LRI	0.989	0.995	0.999

The MSE of the three algorithms are shown in Table 7. NN has the smallest MSE and thus, NN is the most accurate algorithm in this research.

Table 7. MSE results.

Method	Mean Square Error		
	Length (mm)	**Width (mm)**	**Height (mm)**
LR	0.269	0.183	0.0119
LRI	0.118	0.121	0.00532
NN	0.00228	0.0117	0.0000878

5. Verification

In this section, a verification part is sintered to verify the accuracy of the algorithm. Since the MSE of NN is the lowest, the prediction is generated by NN. The manufacturing parameters are shown in Table 8 and the results are shown in the Table 9.

Table 8. The manufacturing parameters of verification part.

Printing Parameter		**Sintering Parameter**	
Layer Thickness (mm)	0.3	Layer Thickness (mm)	0.3
Nozzle Temperature (°C)	220	Sintering Temperature (°C)	880
Printing Speed (mm/s)	15	Ramp Ratio (°C/min)	3

Table 9. Verification of the ML algorithm.

	Target Dimensions	**Predicted CAD Dimensions**	**Final Dimensions after Sintering**
Length (mm)	20	20.905	19.998
Width (mm)	15	15.394	14.996
Height (mm)	6	6.154	6.001

The target final dimensions of this part are 20 mm × 15 mm × 6 mm, and the predictions of CAD size are 20.905 mm × 15.394 mm × 6.154 mm. After the sintering and

polishing, the real final dimensions are 19.998mm × 14.996mm × 6.001 mm. Comparing with the target, the dimensional errors are negligible.

6. Conclusions

AM is one of the latest manufacturing processes that is widely used in several fields. Metal AM is also relatively new and has a potential to be one commonly used low-cost metal manufacturing technologies. Low-cost metal ME does not have the disadvantages of metal AM since it uses metal-infused filament materials instead of pure metal materials. ML can assist researchers to predict the qualities of the parts fabricated by low-cost metal ME. In this research, the printing accuracy and the dimensional changes of low-cost metal ME fabricated parts are analyzed by different algorithms and the following conclusions are drawn:

After the printing process, the non-sintered dimensions are different from the CAD dimensions, it will expand in length and width than the 3D models. As for the height, it will shrink or expand than the 3D models.

- The three types of algorithms behave differently in predicting CAD dimensions. NN has the smallest MSE (0.00228 in length, 0.0117 in width, and 0.0000878 in height) and, hence, will be the best algorithm to predict the initial CAD dimensions.
- Since both LRI and NN have smaller MSE than LR, which means that LRI and NN are more accurate than LR, these independent parameters have internal interactions.
- After verification, the errors between the real and target dimensions are negligible; the accuracy of the prediction by NN is acceptable.
- For NN that more hidden layers can be added to develop deep model that better capture complex behavioral patterns within the data leading to better prediction accuracy. Our results support this claim since the NN gave the best results.

Author Contributions: Conceptualization, I.F. and Z.Z.; methodology, M.I., Z.Z. and J.F.-O.; software, Z.Z. and J.F.-O.; validation, Z.Z.; formal analysis, Z.Z. and J.F.-O.; investigation, Z.Z.; resources, Z.Z.; data curation, Z.Z.; writing—original draft preparation, Z.Z.; writing—review and editing, J.F.-O., M.I., I.F., and M.A.; visualization, Z.Z.; supervision, I.F.; project administration, I.F.; All authors have read and agreed to the published version of the manuscript.

Funding: This research received no external funding.

Data Availability Statement: https://drive.google.com/file/d/1TqlHKQml5DsAWADaSo8g6JCAjHditnaW/view?usp=sharing (accessed on 21 April 2021).

Acknowledgments: This research has been made possible with the help provided by the Additive Manufacturing Research and Innovation Laboratory (Foundation Hall) and Senior Design Laboratory (Brown Hall) in Tennessee Tech University. The technical support provided by Seymur Hasanov and Andy Pardue is greatly appreciated.

Conflicts of Interest: The authors declare no conflict of interest.

References

1. Ngo, T.D.; Kashani, A.; Imbalzano, G.; Nguyen, K.T.; Hui, D. Additive manufacturing (3D printing): A review of materials, methods, applications and challenges. *Compos. Part B Eng.* **2018**, *143*, 172–196. [CrossRef]
2. Zhang, Z.; Fidan, I.; Allen, M. Detection of Material Extrusion In-Process Failures via Deep Learning. *Inventions* **2020**, *5*, 25. [CrossRef]
3. Gibson, I.; Rosen, D.W.; Stucker, B. *Additive Manufacturing Technologies*; Springer: New York, NY, USA, 2014; Volume 17.
4. Redwood, B. Additive Manufacturing Technologies: An Overview. Retrieved 16 April 2018. Available online: https://www.3dhubs.com/knowledge-base/additive-manufacturing-technologies-overview/ (accessed on 21 April 2021).
5. Attaran, M. The rise of 3-D printing: The advantages of additive manufacturing over traditional manufacturing. *Bus. Horiz.* **2017**, *60*, 677–688. [CrossRef]
6. Mohd, J.; Haleem, A. Additive manufacturing applications in medical cases: A literature based review. *Alex. J. Med.* **2018**, *54*, 411–422.
7. Seyed Hamidreza, G.; Corker, J.; Fan, M. Additive manufacturing technology and its implementation in construction as an eco-innovative solution. *Autom. Constr.* **2018**, *93*, 1–11.

8. Berger, R. Additive Manufacturing | Mechanical Engineering | Engineered Products/High Tech | Industrial Know-how | Expertise | Roland Berger. 2013. Available online: https://www.rolandberger.com/publications/publication_pdf/roland_berger_additive_manufacturing_1.pdf (accessed on 21 April 2021).
9. Pinna, C.; Ramundo, L.; Sisca, F.G.; Angioletti, C.M.; Taisch, M.; Terzi, S. Additive Manufacturing applications within Food industry: An actual overview and future opportunities. In Proceedings of the 21st Summer School Francesco Turco, Naples, Italy, 13–15 September 2016.
10. Gisario, A.; Kazarian, M.; Martina, F.; Mehrpouya, M. Metal additive manufacturing in the commercial aviation industry: A review. *J. Manuf. Syst.* **2019**, *53*, 124–149. [CrossRef]
11. Gong, H.; Snelling, D.; Kardel, K.; Carrano, A. Comparison of Stainless Steel 316L Parts Made by FDM-and SLM-Based Additive Manufacturing Processes. *JOM* **2019**, *71*, 880–885. [CrossRef]
12. Oxford English Dictionary. *Edition on CD-ROM (v. 4.0)*; Oxford University Press: Oxford, UK, 2009.
13. Liu, B.; Wang, Y.; Lin, Z.; Zhang, T. Creating metal parts by Fused Deposition Modeling and Sintering. *Mater. Lett.* **2020**, *263*, 127252. [CrossRef]
14. Mohammadizadeh, M.; Lu, H.; Fidan, I.; Tantawi, K.; Gupta, A.; Hasanov, S.; Zhang, Z.; Alifui-Segbaya, F.; Rennie, A. Mechanical and Thermal Analyses of Metal-PLA Components Fabricated by Metal Material Extrusion. *Inventions* **2020**, *5*, 44. [CrossRef]
15. German, R.M. *Sintering Theory and Practice*; Wiley-Interscience: Hoboken, NJ, USA, 1996.
16. Burkhardt, C.; Freigassner, P.; Weber, O.; Imgrund, P.; Hampel, S. Fused filament fabrication (FFF) of 316L Green Parts for the MIM process. In *European Congress and Exhibition on Powder Metallurgy, Proceedings of the European PM Conference Proceedings, Chantilly, France, 9–13 October 2016*; The European Powder Metallurgy Association: Chantilly, France, 2016.
17. Evren, Y.; Ersoy, K. Dimensional Accuracy and Mechanical Properties of Chopped Carbon Reinforced Polymers Produced by Material Extrusion Additive Manufacturing. *Materials* **2019**, *12*, 3885.
18. Silva, D.N.; De Oliveira, M.G.; Meurer, E.; Meurer, M.I.; Da Silva, J.V.L.; Santa-Bárbara, A. Dimensional error in selective laser sintering and 3D-printing of models for craniomaxillary anatomy reconstruction. *J. Cranio-Maxillofac. Surg.* **2008**, *36*, 443–449. [CrossRef]
19. Danilo, I.; Broilo, T.L.; Heitz, C.; de Oliveira, M.G.; de Oliveira, H.W.; Nobre, S.M.; Dos Santos Filho, J.H.; Silva, D.N. Dimensional error of selective laser sintering, three-dimensional printing and PolyJet™ models in the reproduction of mandibular anatomy. *J. Cranio Maxillofac. Surg.* **2009**, *37*, 167–173.
20. Wang, Y.; Zhao, Y.F. Investigation of sintering shrinkage in binder jetting additive manufacturing process. *Procedia Manuf.* **2017**, *10*, 779–790. [CrossRef]
21. Bustillo, A.; Pimenov, D.; Matuszewski, M.; Mikolajczyk, T. Using artificial intelligence models for the prediction of surface wear based on surface isotropy levels. *Robot. Comput. Integr. Manuf.* **2018**, *53*, 215–227. [CrossRef]
22. Zhou, L.; Pan, S.; Wang, J.; Vasilakos, A.V. Machine learning on big data: Opportunities and challenges. *Neurocomputing* **2017**, *237*, 350–361. [CrossRef]
23. Zhou, Z.; Chen, K.; Li, X.; Zhang, S.; Wu, Y.; Zhou, Y.; Meng, K.; Sun, C.; He, Q.; Fan, W.; et al. Sign-to-speech translation using machine-learning-assisted stretchable sensor arrays. *Nat. Electron.* **2020**, *3*, 571–578. [CrossRef]
24. Nugrahaeni, R.A.; Mutijarsa, K. Comparative analysis of machine learning KNN, SVM, and random forests algorithm for facial expression classification. In Proceedings of the 2016 International Seminar on Application for Technology of Information and Communication (ISemantic), Piscataway, NJ, USA, 5–6 August 2016; IEEE: New York, NY, USA, 2016.
25. Cammarota, G.; Ianiro, G.; Ahern, A.; Carbone, C.; Temko, A.; Claesson, M.J.; Gasbarrini, A.; Tortora, G. Gut microbiome, big data and machine learning to promote precision medicine for cancer. *Nat. Rev. Gastroenterol. Hepatol.* **2020**, 1–14. [CrossRef]
26. Bayraktar, Ö.; Uzun, G.; Çakiroğlu, R.; Guldas, A. Experimental study on the 3D-printed plastic parts and predicting the mechanical properties using artificial neural networks. *Polym. Adv. Technol.* **2017**, *28*, 1044–1051. [CrossRef]
27. Hedberg, T.D., Jr.; Hartman, N.W.; Rosche, P.; Fischer, K. Identified research directions for using manufacturing knowledge earlier in the product life cycle. *Int. J. Prod. Res.* **2017**, *55*, 819–827. [CrossRef]
28. Noriega, A.; Blanco, D.; Alvarez, B.J.; Garcia, A. Dimensional accuracy improvement of FDM square cross-section parts using artificial neural networks and an optimization algorithm. *Int. J. Adv. Manuf. Technol.* **2013**, *69*, 2301–2313. [CrossRef]
29. The Virtual Foundary. Available online: https://shop.thevirtualfoundry.com/collections/metal-filaments/products/bronze-filamet?variant=12351189483603 (accessed on 21 April 2021).
30. Ultimaker S5 PDF User Manuals. Available online: https://support.ultimaker.com/hc/en-us/articles/360011654419-Ultimaker-S5-PDF-user-manuals (accessed on 21 April 2021).
31. MTI Corporation. Available online: https://www.mtixtl.com/1100CCompactMuffleFurnacewith30SegmentProgrammable-KSL-1100X-S-UL.aspx (accessed on 9 January 2021).
32. iGaging. Available online: http://www.igaging.com/page73.html (accessed on 21 April 2021).
33. Chen, J.; de Hoogh, K.; Gulliver, J.; Hoffmann, B.; Hertel, O.; Ketzel, M.; Bauwelinck, M.; van Donkelaar, A.; Hvidtfeldt, U.A.; Katsouyanni, K.; et al. A comparison of linear regression, regularization, and machine learning algorithms to develop Europe-wide spatial models of fine particles and nitrogen dioxide. *Environ. Int.* **2019**, *130*, 104934. [CrossRef]
34. Uyanık, G.K.; Güler, N. A study on multiple linear regression analysis. *Procedia Soc. Behav. Sci.* **2013**, *106*, 234–240. [CrossRef]
35. Hayes, A.F.; Montoya, A.K. A tutorial on testing, visualizing, and probing an interaction involving a multicategorical variable in linear regression analysis. *Commun. Methods Meas.* **2017**, *11*, 1–30. [CrossRef]

36. Zhang, P.; Shen, H.; Zhai, H. Machine learning topological invariants with neural networks. *Phys. Rev. Lett.* **2018**, *120*, 066401. [CrossRef] [PubMed]
37. Mao, H.; Han, S.; Pool, J.; Li, W.; Liu, X.; Wang, Y.; Dally, W.J. Exploring the regularity of sparse structure in convolutional neural networks. *arXiv* **2017**, arXiv:1705.08922.
38. Zhang, Z. Detection of the Additive Manufacturing In-Process Failures via Deep Learning. Master's Thesis, Tennessee Technological University, Cookeville, TN, USA, 2019.
39. Di Leo, G.; Sardanelli, F. Statistical significance: *p* value, 0.05 threshold, and applications to radiomics—Reasons for a conservative approach. *Eur. Radiol. Exp.* **2020**, *4*, 1–8.
40. Cuadras, C.M. Increasing the correlations with the response variable may not increase the coefficient of determination: A PCA interpretation. In *Multivariate Statistics and Matrices in Statistics*; De Gruyter: Berlin, Germany, 2020; pp. 75–84.
41. Nicolson, A.; Paliwal, K.K. Deep learning for minimum mean-square error approaches to speech enhancement. *Speech Commun.* **2019**, *111*, 44–55. [CrossRef]